Journal of Geosciences, 63 (2018), 317–331 DOI: 10.3190/jgeosci.278

Original paper

Petrology of weakly differentiated alkaline, high-level intrusive rocks in the Zahořany–Chotiněves Belt near Litoměřice (Czech Republic)

Jakub MYSLIVEČEK[1,2], Vladislav RAPPRICH[1]*, Yulia V. KOCHERGINA[1,3], Tomáš MAGNA[1], Patricie HALODOVÁ[1], Zoltán PÉCSKAY[4], Michal POŇAVIČ[1]

[1] *Czech Geological Survey, Klárov 3, 118 21 Prague 1, Czech Republic; vladislav.rapprich@geology.cz*
[2] *Institute of Petrology and Structural Geology, Faculty of Science, Charles University, Albertov 6, 128 43 Prague 2, Czech Republic*
[3] *Institute of Geochemistry and Mineral Resources, Faculty of Science, Charles University, Albertov 6, 128 43 Prague 2, Czech Republic*
[4] *Institute for Nuclear Research (ATOMKI), Hungarian Academy of Sciences, Bem tér 18/C, 4001 Debrecen, Hungary*
[*] *Corresponding author*

Weakly differentiated rocks such as basaltic trachyandesites occur rather rarely in the Cenozoic České Středohoří Volcanic Complex (Central Europe, Czech Republic). We present mineralogical, petrological and geochemical data for a basaltic trachyandesite sill located at the southern margin of the České Středohoří Volcanic Complex, where several smaller hills form a quasi-continuous belt between villages of Zahořany and Chotiněves. Uniform petrography and chemical composition provide compelling evidence that all individual outcrops belong to a single large sill, probably with the exception of the westernmost occurrence at the Křemín Hill. The sill is almost 5 km long (SW–NE) and likely up to 3 km wide (NW–SE). The elongated shape of the sill and its position suggest that the basaltic trachyandesite magma ascended along the Litoměřice Fault forming the south-eastern edge of the NE–SW trending Ohře (Eger) Rift.

The studied rocks are basic and alkali-rich (49.5–50.3 wt. % SiO_2, sum $K_2O + Na_2O$ = 7.8–8.1 wt. %), but their silica contents (volatile-free) approach the boundary of the intermediate domain. This correlates with low concentrations of compatible trace elements such as Cr (15–23 ppm). The limited degree of differentiation is reflected by smooth chondrite-normalized REE patterns (La_N/Yb_N = 18.2–19.3) with the absence of any significant Eu and/or MREE anomaly. The incompatible trace-element contents (Sr = 920–1080 ppm, Ba = 840–950 ppm, ΣREE = 280–330 ppm) typify weakly differentiated alkaline volcanic rocks within the Ohře Rift. Based on the chemical composition we suggest that these basaltic trachyandesites belong to the České Středohoří Volcanic Complex rather than to MgO-poor foidites of the Central Bohemia Volcanic Field. The intrusive age of the sill has been determined using conventional whole-rock K–Ar method at 29.12 ± 0.63 Ma (1σ). The initial Sr–Nd isotope compositions ($^{87}Sr/^{86}Sr_i$ = 0.7048, $^{143}Nd/^{144}Nd_i$ = 0.51270), compare well with existing data for the České Středohoří trachybasalts and attest to their common origin. The single large Zahořany–Chotiněves sill partly fills the apparent gap in the differentiation trend between basanites to trachybasalts and trachyandesites to phonolites reported for the alkaline volcanism of the České Středohoří Mts.

Keywords: basaltic trachyandesite, Zahořany–Chotiněves sill, České Středohoří Volcanic Complex, petrology, Sr–Nd isotopes, K–Ar dating
Received: 9 February 2018; accepted: 17 December 2018; handling editor: B. van Wyk de Vries
The online version of this article (doi: 10.3190/jgeosci. 278) contains supplementary electronic material.

1. Introduction

Differentiation of alkaline rocks and petrogenesis of trachytes and phonolites remain the subject of debate (e.g., Le Roex et al. 1990; Simonsen et al. 2000; Legendre et al. 2005; Jung et al. 2013; Ackerman et al. 2015; Büchner et al. 2015). Unfortunately, many of the alkaline igneous complexes and volcanic fields tend to produce bimodal suites represented by both primitive (olivine nephelinites, basanites, trachybasalts) and highly differentiated rocks (trachytes, phonolites, alkali rhyolites) with a gap in between, known as the Daly gap (Daly 1914; Clague 1978). However, the understanding of the complex processes leading to formation of differentiated alkaline melts can be facilitated if complete differentiation path is preserved in eruptive sequences associated with a single common source (e.g., Maury et al. 1980; Villemant et al. 1980, 1981; Hamelin et al. 2009; Ulrych et al. 2016).

A group of separate hills forms a ~5 km long belt on the south-eastern margin of the České Středohoří Volcanic Complex (CSVC) between villages Zahořany and Chotiněves (Fig. 1). Even though these hills were recognized to be built by trachybasalts to trachyandesites (Domas ed. 1988), they were never a focus of any detailed petrological study. Furthermore, their tectonic position at the Litoměřice Fault is dubious. The entire group could belong either to the České Středohoří Volcanic Complex occupying central part of the Ohře (Eger) Rift (Cajz et al. 1999, 2009; Ulrych et al. 2002), or the compositionally distinct Central Bohemia Volcanic Field (Ulrych et al. 1998; Řanda et al. 2003; Jáklová et al. 2014).

The aims of this study were (i) to constrain the geochemical affinity of the studied rocks to one of these magmatic systems, and (ii) to characterize the evolution of differentiated alkaline rocks.

2. Geological setting

The Bohemian Massif in Central Europe experienced extensive magmatic/volcanic activity in several periods during the Cenozoic (e.g., Ulrych et al. 2011 and references therein). Most of the magmatism was concentrated along the Ohře (Eger) Rift, which forms the NE branch of the European Cenozoic Rift System (Dèzes et al. 2004). The Ohře Rift runs across the western part of the Bohemian Massif in the ENE–WSW direction, roughly following the Variscan suture between the Saxothuringian and Teplá–Barrandian domains of the Bohemian Massif (see Mlčoch and Konopásek 2010). The Cenozoic magmatism of the Bohemian Massif represents an important part of much wider alkaline circum-Mediterranean anorogenic Cenozoic igneous province (Lustrino and Wilson 2007).

Two main volcanic complexes – České Středohoří and Doupovské hory volcanic complexes – have emerged within the Ohře Rift (e.g., Cajz et al. 1999, 2009; Ulrych et al. 2002; Rapprich and Holub 2008; Holub et al. 2010; Skála et al. 2014; Ackerman et al. 2015). The formation of these major volcanic complexes was paralleled by scattered monogenetic volcanism in several volcanic fields on both rift-shoulders (e.g., Awdankiewicz 2005; Rapprich et al. 2007; Büchner and Tietz 2012; Valenta et al. 2014; Petronis et al. 2015; Tietz and Büchner 2015; Awdankiewicz et al. 2016; Haase et al. 2017; Wenger et al. 2017).

Activity of the *České Středohoří Volcanic Complex* lasted from the Late Eocene until the Late Miocene and its eruptive products represent a sequence of four formations (Cajz et al. 1999, 2009; Ulrych et al. 2002): basanitic Ústí Fm. (36.1–25.5 Ma), trachybasaltic Děčín Fm. (30.8–24.7 Ma), basanitic Dobrná Fm. (24.0–19.3 Ma), and basanitic Štrbice Fm. (13.9–9.0 Ma), respectively. The Roztoky Intrusive Complex, representing the main feeding system, was emplaced in the central part of the České Středohoří Volcanic Complex in the Early Oligocene (Skála et al. 2014). Within the Roztoky Intrusive Complex, Rapprich et al. (2017a) recently documented a minor intrusion of silicocarbonatite, which are often associated with alkaline silicate magmatism (e.g., Le Bas 1977; Wooley and Kjarsgaard 2008; Stoppa and Schiazza 2013). According to Ackerman et al. (2015), the trachybasalts were derived from basanites of the Ústí Fm. through 6–42 % fractional crystallization of 20 % olivine and 80 % clinopyroxene from the parental basanitic magma. The fractionation was associated, to some extent, with assimilation, with the mass ratio of assimilation/fractional crystallization estimated at 0.6. Further crystal fractionation associated with assimilation of crustal rocks produced trachytic and phonolitic magmas.

The České Středohoří Volcanic Complex fills the central segment of the Ohře Rift. In this sector, the Ohře Rift is truncated by the Litoměřice Fault (*syn.* České Středohoří Fault; Cajz and Valečka 2010, and references therein) in the south. The scattered occurrences of volcanic rocks on the southern rift-shoulder (south of the Litoměřice Fault) are known as the *Central Bohemia Volcanic Field* and are characterized by generally lower MgO and higher P_2O_5 contents compared with the České Středohoří Volcanic Complex proper (Ulrych et al. 1998; Řanda et al. 2003; Jáklová et al. 2014).

This study investigates the belt of flat-top hills between the villages Zahořany and Chotiněves near Litoměřice (Fig. 1). This belt is parallel to the Litomeřice Fault, but located south of the fault on an uplifted shoulder. The hills consist of basaltic trachyandesite, which intruded as a sill into clayey-glauconitic sandstones of the Jizera Formation (Middle to Upper Turonian), marlstones and limestones of the Teplice Formation (Upper Turonian to Lower Coniacian) and claystones to marlstones of the Březno Formation (Coniacian) of the Bohemian Cretaceous Basin (Domas 1988). Erosional relics of porcelanites representing remnants of original sedimentary mantle of the intrusion are dispersed over the surface of the volcanic body. Individual hills were originally mapped as separate bodies (Domas 1988; Valečka et al. 2002).

3. Methods

The detailed study of the Zahořany–Chotiněves basaltic trachyandesite belt started with the new field mapping of the area, involving also sampling.

3.1. Ground magnetometric survey

Variations of magnetic field over the entire area were systematically mapped to localize the feeding conduit(s) of the studied volcanic belt. Efficiency of this method for the detection of basaltic volcanic conduits has been confirmed worldwide (e.g., De Ritis et al. 2005; Skácelová et al. 2010; Blaikie et al. 2014; Marshall et al. 2015). The field magnetic data were acquired using a PMG-2 Proton precession magnetometer (Geofyzika Brno) in the mode of separated individual measurements. The variations

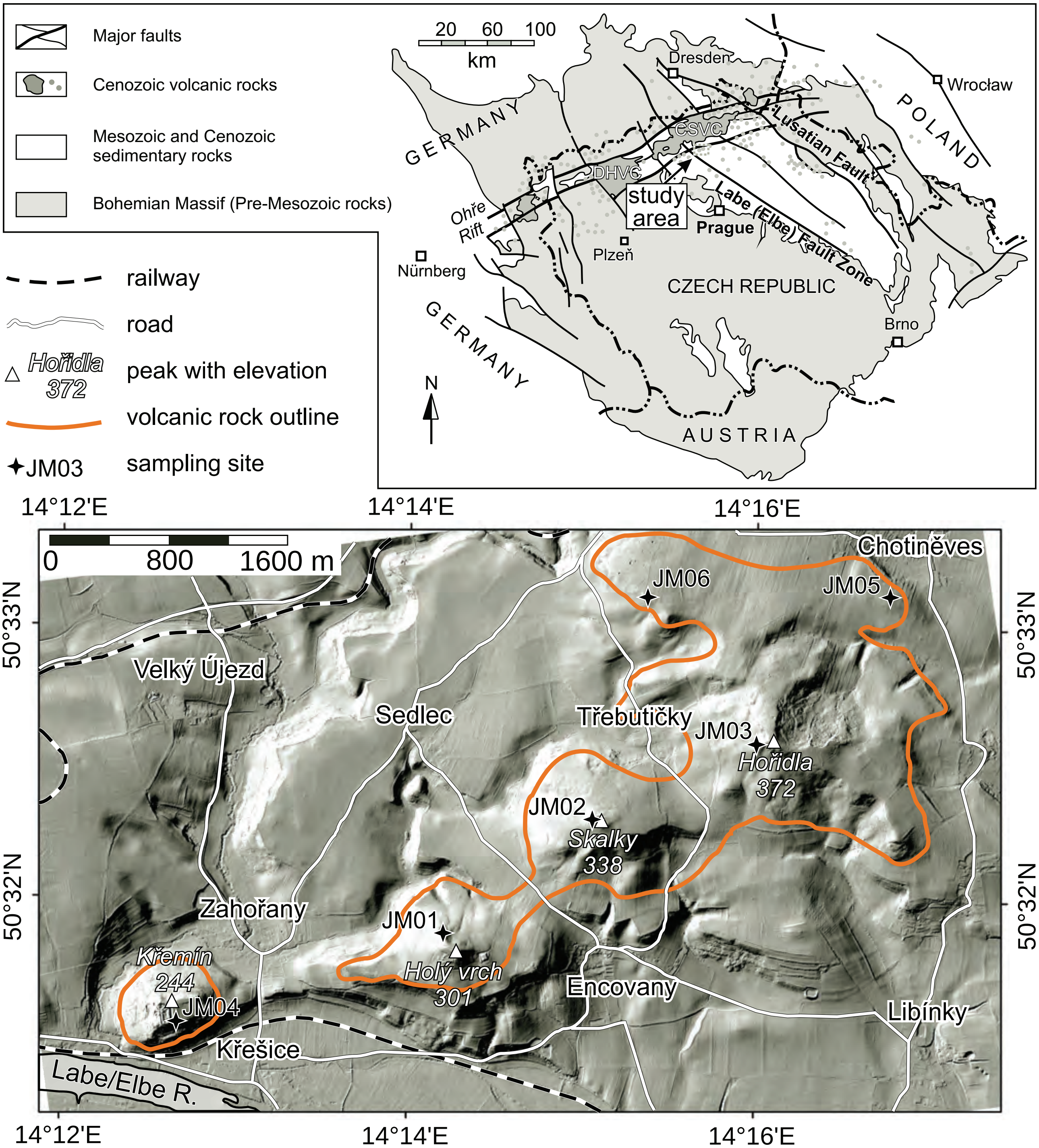

Fig. 1 Schematic map of the studied locality and its relation to the Ohře Rift and Labe (Elbe) Fault zone (**a**). CSVC – České Středohoří Volcanic Complex; DHVC – Doupovské Hory Volcanic Complex. Location of the studied belt of basaltic trachyandesites between Zahořany and Chotiněves (**b**).

of magnetic field were measured along several profiles, with additional measurements added, where magnetic anomaly was expected. Each measurement was individually localized using GPS. The total magnetic field in the area according to the World Magnetic Model (Chulliat et al. 2015) should be *c*. 49,100 nT.

3.2. Petrology and mineral chemistry

The thin-section investigations were made by a petrographical microscope Nikon Eclipse E200. The quantitative chemical analyses of individual mineral phases were performed using a Tescan MIRA 3GMU electron

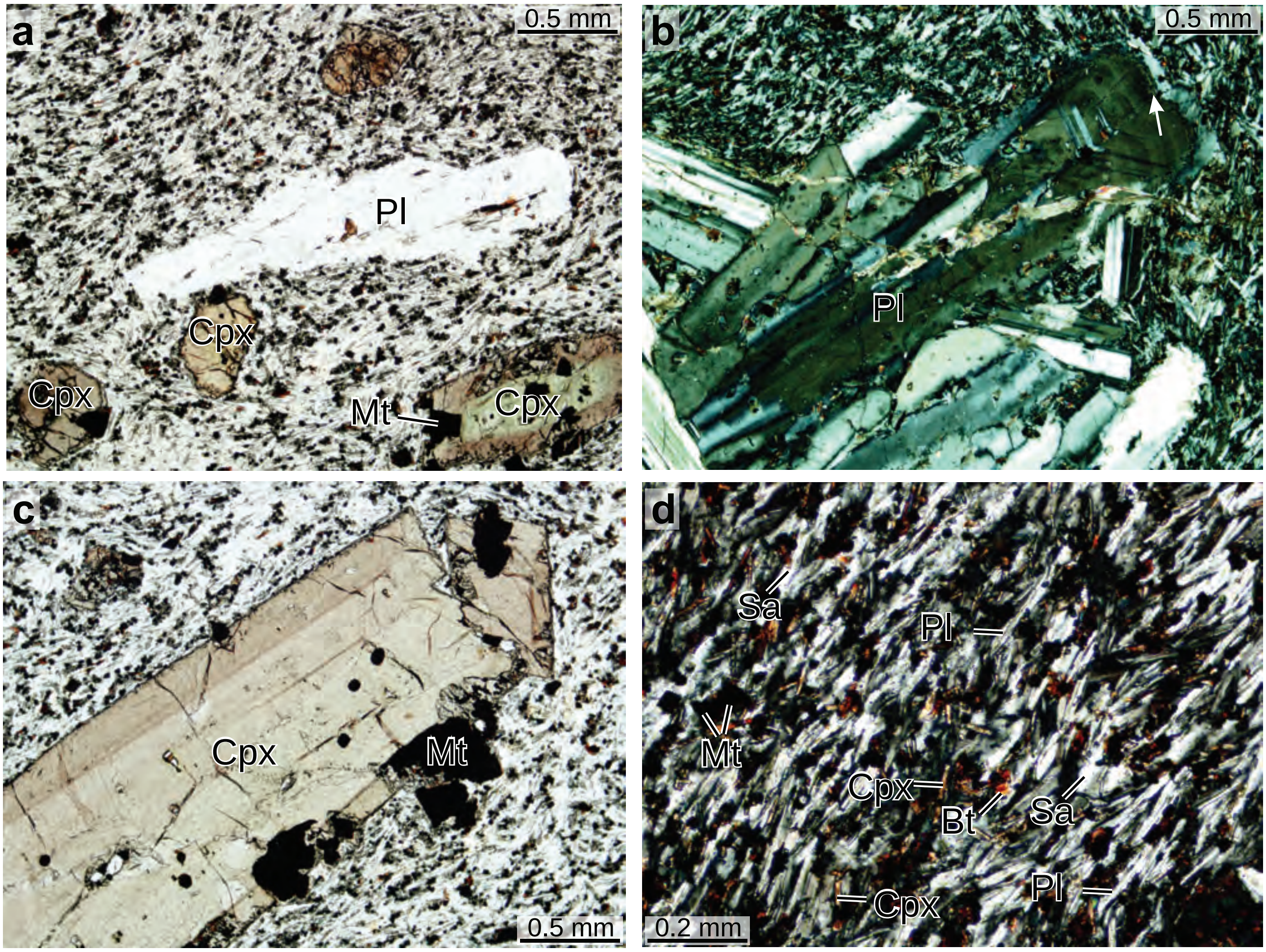

Fig. 2 Photomicrographs of the studied rocks: **a** – Plagioclase and clinopyroxene phenocrysts in fine-grained groundmass (JM01; plane-polarized light); **b** – Plagioclase glomerocryst with oscillatory zoning, arrow points to a corona of inclusions (JM01; cross-polarized light); **c** – Zoned clinopyroxene phenocryst (JM02; plane-polarized light); **d** – Close-up on the groundmass consisting of plagioclase, sanidine, clinopyroxene, biotite and magnetite (JM02; cross-polarized light). Bt – biotite, Cpx – clinopyroxene, Mt – magnetite, Pl – plagioclase, Sa – sanidine.

microprobe fitted with SDD X-Max 80 mm^2 EDS detector and AZtecEnergy software (Oxford Instruments), housed at the Czech Geological Survey, Prague. Point analyses and the area analyses of selected minerals and parts of the sample were acquired using the following conditions: accelerating voltage 15 kV, working distance 15 mm, 3 nA probe current, 30 s acquisition time. The SPI mineral set of standards was used for standardization.

3.3. Bulk-rock chemistry

The collected fresh samples were crushed and pulverized in an agate mortar. Geochemical analyses of three selected rock samples were performed at the Czech Geological Survey, Prague. The major-element analysis followed the methods described by Dempírová et al. (2010) including atomic absorption spectrometry, photometry and titration with Complexon III.

Trace-element concentrations were determined with an Agilent 7900x ICP-MS, housed at the Czech Geological Survey, following dissolution in a mixture of concentrated HNO_3–HF and equilibration with HCl. Reference basalt BHVO-2 (USGS) and syenite JSy-1 (GSJ) were analyzed together with unknown samples. Their results were consistent with the published data within ± 10 % for most elements (Jochum et al. 2005, see Electronic supplementary material – ESM 1).

3.4. K–Ar geochronology

The K–Ar age determination of sample JM02 was performed in the ATOMKI Laboratories, Debrecen, Hungary. The sieved bulk-rock fraction 0.1–0.3 mm was repeatedly washed in distilled water prior to further analytical procedures. Following acid digestion and 0.2 M HCl dissolution of the samples, the potassium content was determined by flame photometry using a Model 420 Industrial with a Na buffer and Li internal standard. Measurements were checked by inter-laboratory standards (Asia 1/65, LP-6, HD-B1 and GL-O). Argon was extracted from the samples by high-frequency fusion in Mo crucible under vacuum conditions. A ^{38}Ar-spike was added to samples prior to gas-cleaning in Ti-sponge and SAES St 707 type and liquid nitrogen traps, respectively. The Ar isotope ratios were measured in the static mode using a 15 cm radius magnetic sector-type mass spectrometer built in ATOMKI in Debrecen (see Odin 1982 and Balogh 1985 for details). Age calculations were based on constants proposed by Steiger and Jäger (1977) and the results of K–Ar dating are given with 1σ errors.

3.5. Sr–Nd isotope data

A representative sample JM02 was selected for the Sr–Nd isotope analysis. The analytical details for sample processing and ion-exchange chemistry for Sr and Nd separation are described in Walther et al. (2016). Strontium and Nd isotope analyses were performed using a Triton Plus thermal ionization mass spectrometer (TIMS; Thermo Fisher) housed at the Czech Geological Survey, Prague. Strontium isotope composition was measured in a static mode using a single Ta filament whereas Nd isotope composition was measured in a dynamic mode using a double Re filament assembly. The ^{143}Nd/^{144}Nd and ^{87}Sr/^{86}Sr ratios were corrected for mass fractionation assuming ^{146}Nd/^{144}Nd = 0.7219 and ^{86}Sr/^{88}Sr = 0.1194, respectively. External reproducibility was estimated from replicate analyses of the NBS 987 (Pin et al. 2014: ^{87}Sr/^{86}Sr = 0.710241 ± 12; results from this study: ^{87}Sr/^{86}Sr = 0.710253 ± 9, 2σ; n = 30, static mode) and JNdi-1 (Pin et al. 2014: ^{143}Nd/^{144}Nd = 0.512103 ± 2; results from this study: ^{143}Nd/^{144}Nd = 0.512110 ± 8, 2σ; n = 7, dynamic mode) reference materials. The initial Sr–Nd isotope ratios (29 Ma; this study) were calculated using decay constants given by Steiger and Jäger (1977: $\lambda_{Rb} = 1.42 \times 10^{-11}$) and Lugmair and Marti (1978: $\lambda_{Sm} = 6.54 \times 10^{-12}$), respectively. The ε_{Nd} values were obtained using Bulk Earth parameters of Jacobsen and Wasserburg (1980). The reliability of Sr–Nd methods was monitored by the analyses of JB-3 reference basalt (^{87}Sr/^{86}Sr = 0.703449 ± 8, ^{143}Nd/^{144}Nd = 0.513032 ± 11), that were in agreement with published data (Pin et al. 2014: ^{143}Nd/^{144}Nd = 0.513049 ± 3, ^{87}Sr/^{86}Sr = 0.703422 ± 9).

4. Results

4.1. Geology and petrography

During detailed geological mapping of the area, small outcrops and dispersed blocks of basaltic trachyandesite were newly documented also in the saddles between individual elevations (ESM 2). Thus, the individual bodies seem interconnected. The Cretaceous sediments within the bounds of the volcanic body, if present, are represented by porcelanites rather than intact marlstones. The presence of porcelanites suggests proximity of volcanic rock as a source of heat underneath. In addition, digital elevation model based on 5th generation LiDAR (provided by the State Administration of Land Surveying and Cadastre of the Czech Republic; Fig. 1) was used to improve geometry of the intrusive body. The only exception is the westernmost Křemín Hill (JM04), representing an isolated occurrence. The geometry of the Křemín Hill was significantly modified by construction of early medieval fortification. However, no outcrops were found on this elevation, and frequent fragments of basaltic rocks might be derived from the fortification walls. Therefore, this site was sampled only for thin section investigations and electron-microprobe studies.

In the remaining part of the belt, five principal outcrops were found and sampled for thin sections; three macroscopically freshest outcrops were sampled also for geochemistry. Most samples from the entire belt have identical composition of a basaltic trachyandesite varying solely in the degree of weathering. The only exception is Křemín Hill (JM04) with sanidine prevailing over plagioclase, slightly lower amount of clinopyroxene and higher amount of magnetite compared with the other samples. All other studied rocks are dominated by plagioclase, which prevails in the groundmass, but also forms euhedral to subhedral phenocrysts up to 3 mm (Fig. 2a). The largest plagioclase phenocrysts were observed in sample JM01, where plagioclase crystals tend to form glomerocrysts up to 5 mm in size (Fig. 2b). The larger plagioclase phenocrysts display oscillatory zoning, with the outermost growth zone marked by a corona of inclusions (Fig. 2b).

Clinopyroxene phenocrysts are more abundant than plagioclase ones but still represent only ~5 vol. % of the rock. They are euhedral, up to 3.5 mm across, and consist of up to three optically visible growth zones. The outermost growth zone is marked with frequent magnetite inclusions (Fig. 2c). Sanidine phenocrysts occur scarcely with a size not exceeding 1.2 mm. Biotite is pleochroic from ochre (direction α) to brown (direction β or γ) colour and adopts the preferred orientation of groundmass.

Pseudomorphs after amphibole (up to 2 mm) consist of clinopyroxene, magnetite, biotite and, to a lesser extent, plagioclase and analcime. Occasionally, a pseudomorph after quartz (1 mm across) replaced by a mixture of clinopyroxene and plagioclase was observed.

Euhedral plagioclase (up to 0.4 mm) dominates over sanidine in the groundmass in all samples, except for JM04. Both feldspar types display a strong preferred

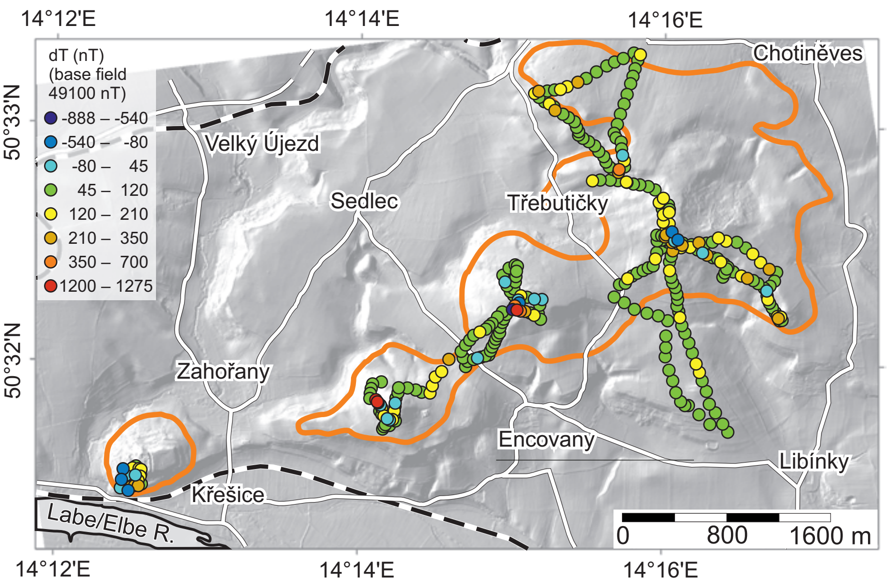

Fig. 3 Ground magnetometry data, showing position of the principal anomalies, plotted over the Digital Elevation Model of the studied area.

orientation (Fig. 2d). Brownish subhedral clinopyroxene (up to 0.2 mm) with magnetite (up to 0.1 mm) frequently occur in the groundmass. The spaces between smaller crystals are filled with anhedral analcime. Apatite, which is the main accessory phase, was not observed optically (due to its size) but it was detected during microprobe survey. Cracks in the rocks are filled with small amounts of secondary calcite.

4.2. Ground magnetic survey

Ground magnetometry data are presented in the ESM 3, and visualized on map (Fig. 3). The overall magnetic image is plain, generally with only weak anomalies of low amplitudes (on the order of several hundreds nT in both positive and negative values). Stronger anomalies (up to 1,275 nT) with sharp boundaries were detected only on the western slope of the Holý vrch Hill and on the summit of the Skalky Hill (Fig. 3). On the other hand, no significant anomaly was detected in the area of apical plateau of the Hořidla Hill. Only negligible variations were detected in this most extensive occurrence. The magnetic image of the Křemín Hill is characterized by moderate (up to 430 nT), sharply bordered anomalies.

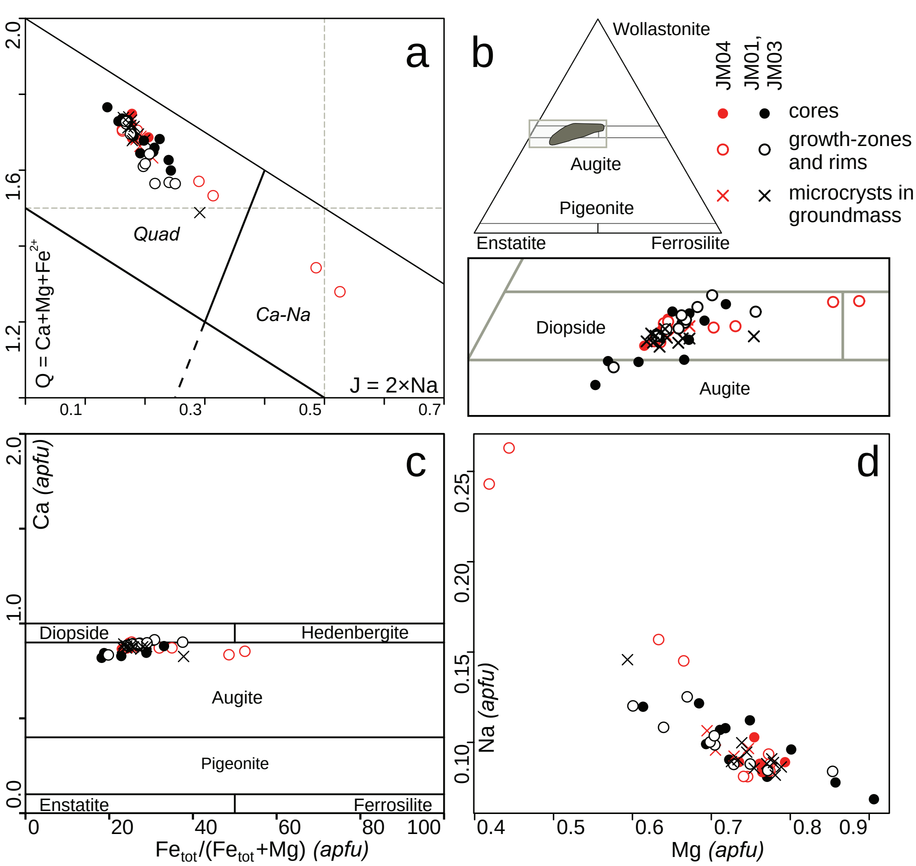

4.3. Mineral chemistry

Clinopyroxene Composition of studied clinopyroxenes (ESM 4) varies along a relatively short differentiation trend

Fig. 4 Composition of clinopyroxenes in the studied samples: **a** – Q–J diagram (Morimoto 1988); **b** – Quadrilateral En–Fs–Wo diagram (mol. %; Morimoto 1988); **c** – Classification diagram based on apfu values of Fe, Mg and Ca (Rapprich 2005); **d** – Binary diagram Mg *vs.* Na (apfu).

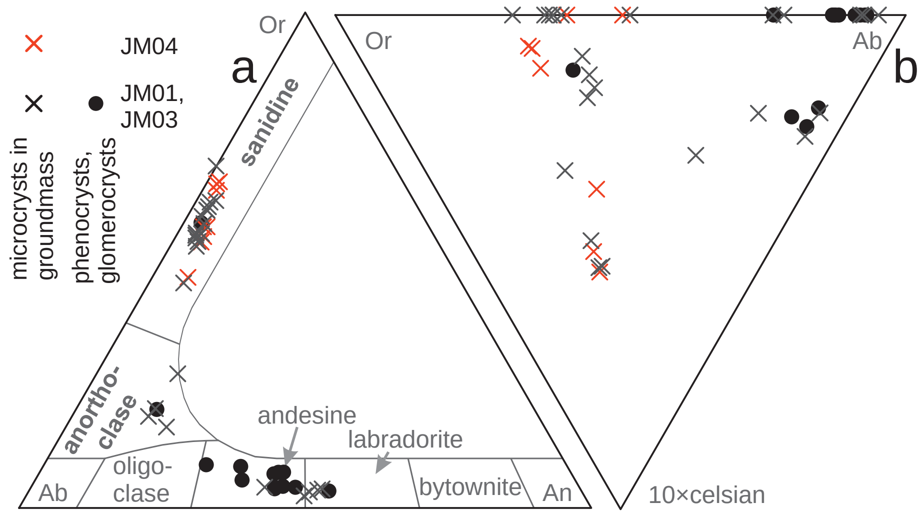

Fig. 5 Composition of feldspars in the studied rocks (mol %): **a** – Classification of feldspars; **b** – Ternary diagram of alkali feldspars including celsian (Ba-feldspar).

(0.25–0.35 Mg apfu, atoms per formula unit). More evolved clinopyroxenes were observed in petrographically slightly different sample JM04. Most of the analyzed compositions fall into the Quad field in the Q–J classification diagram (Morimoto 1988; Fig. 4a), and therefore the quadrilateral diagram (Morimoto 1988; Fig. 4b) was applied. Only the outer rims of the pyroxene phenocrysts in the sample JM04 plot into the field of Ca–Na pyroxenes.

In the quadrilateral diagram (Fig. 4b), the analyzed samples cluster predominantly in the diopside field, and should be classified as ferroan diopsides according to the IMA nomenclature. In contrast, the true Ca content mostly does not exceed 0.9 apfu, suggesting that the clinopyroxenes correspond compositionally rather to augites (Fig. 4c). The overestimated wollastonite component in the quadrilateral diagram is an effect of high amount of Ca-Tschermak's molecules admixture common in clinopyroxenes of alkaline rocks (Rapprich 2005). The outer rims of larger phenocrysts in the sample JM04 correspond to aegirine–augite (Fig. 4a, c) with the content of sodium increasing to ~0.25 apfu (Fig. 4d). Composition of the fine-grained groundmass clinopyroxene microcrysts corresponds to the outer parts of the larger phenocrysts. In several cases, reverse zoning (Mg-enriched rim compared to the phenocryst core) may suggest some role of magma replenishment during formation of the sill.

Feldspars A wide compositional range was observed in the studied feldspars (ESM 5). Larger phenocrysts and crystals in glomerocrysts have a composition of labradorite to andesine. From these early formed calcic members, microcrysts in the matrix show a continuous trend via oligoclase and anorthoclase towards sanidine (Fig. 5a). All feldspars analyzed in the sample JM04 (no larger phenocrysts or glomerocrysts present) plot into the field of sanidine. In some feldspars, a significant Ba content was detected (up to 0.02 apfu; 1.2 wt. %). No clear systematics between Ba content and type/size of feldspar was observed (Fig. 5b).

Magnetite Rather homogeneous composition was documented in the analysed Ti-magnetites (ESM 6, Fig. 6a). In addition, magnetite from the sample JM04 does not differ from magnetite in the other samples. Slight variation can be observed in the concentrations of Al, Mg, and to lesser extent also Mn. A significant decrease in Mg and slight increase in Mn can be observed from larger crystals and inclusions enclosed in clinopyroxene and feldspar towards microcrysts in groundmass (Fig. 6b). The decrease in Mg is associated with decreasing Al, following a trend at Al:Mg ratio 3 : 2 to 1 : 1 (Fig. 6c). Such a trend indicates a role of spinel admixture (up to 15 mol. %) during early crystallization of magnetite.

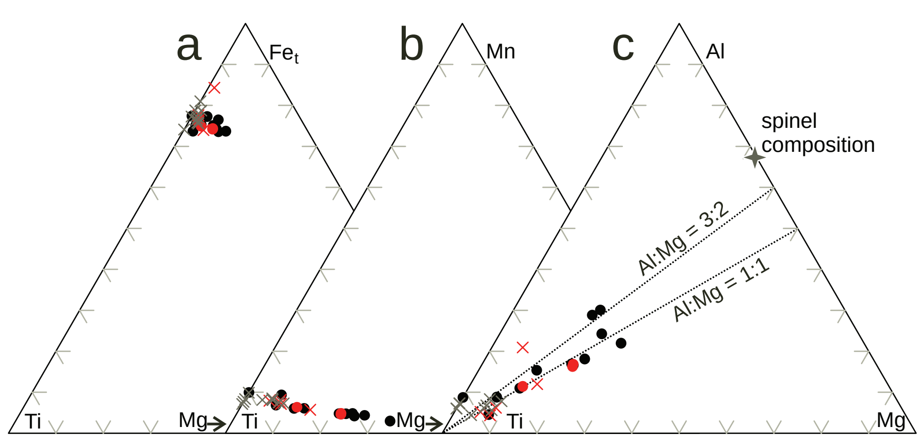

Fig. 6 Composition of magnetites in ternary diagrams: **a** – Ti–Fe_t–Mg; **b** – Ti–Mn–Mg; **c** – Ti–Al–Mg. All values in apfu.

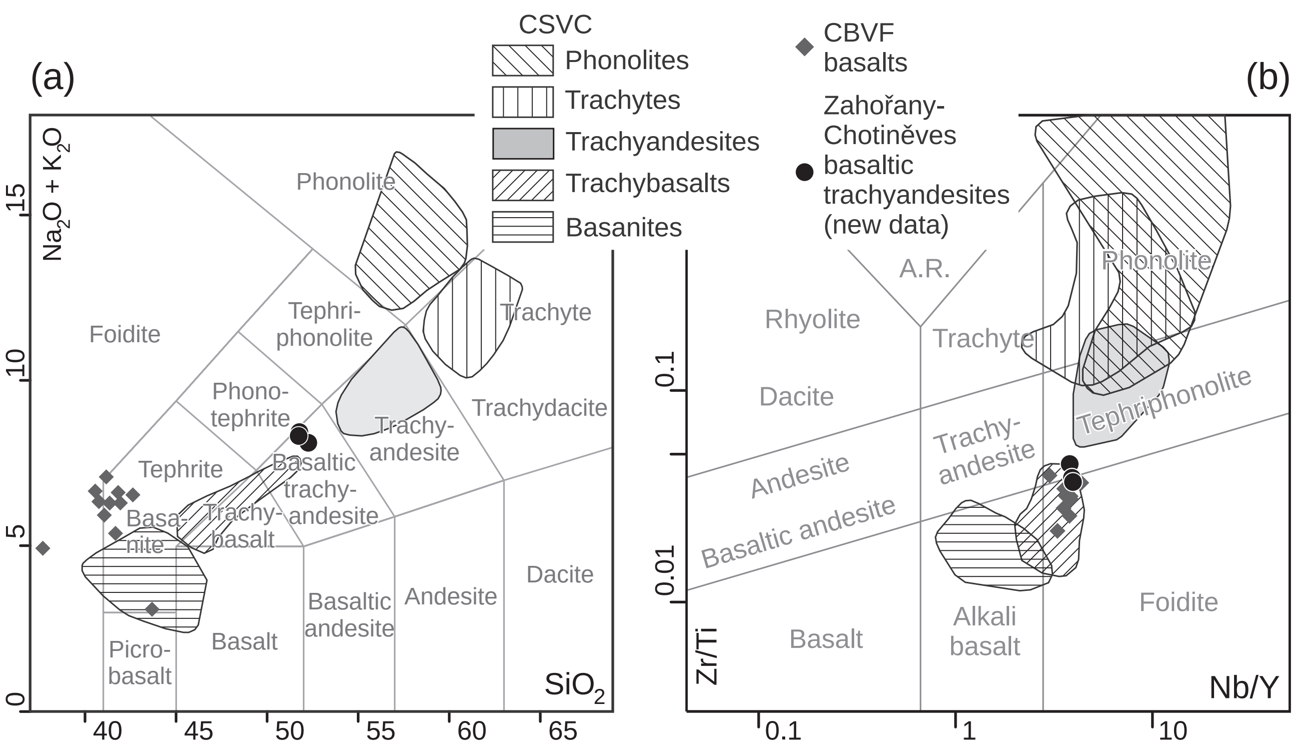

Fig. 7 Classification of the studied rocks: **a** – TAS diagram (Le Maitre et al. 2002); **b** – Nb/Y vs. Zr/Ti classification plot (Pearce 1996). A.R. = Alkali rhyolite. Data from České Středohoří Volcanic Complex (CSVC; Ulrych et al. 2002; Ackerman et al. 2015) and Central Bohemia Volcanic Field (CBVF; Ulrych et al. 1998; Řanda et al. 2003; Jáklová et al. 2014) are also plotted.

4.4. Bulk-rock chemistry

The analysed rocks are relatively fresh, compared to other Cenozoic alkaline rocks of the wider area, with H_2O_{tot} content varying in the range 3.2–3.8 wt. %, and $CO_2 \leq$ 0.15 wt. %. They are basic and alkali-rich (49.5–50.3 wt. % SiO_2, sum $K_2O + Na_2O$ = 7.8–8.1 wt. %), but their silica contents (volatile-free) approach the boundary of the intermediate domain. In the TAS classification diagram, all samples cluster into the field of basaltic trachyandesite (Le Maitre et al. 2002; Fig. 7a). Chemical variations among individual samples are negligible (Tabs 1 and 2). The studied rocks partly fill the gap in the differentiation trend of the CSVC rocks. They project at the boundary between foidite and tephriphonolite fields in the Nb/Y vs. Zr/Ti diagram (Pearce 1996; Fig. 7b). Foidites of the Central Bohemia Volcanic Field (CBVF) differ from the České Středohoří Volcanic Complex (including new data from this study) in having higher contents of alkalis at given silica content (Fig. 7a), despite sharing comparable Nb/Y ratios (Fig. 7b). The contents of P_2O_5 (0.53–0.56 wt. %), Sr (920–1,080 ppm), Ba (840–950 ppm), and ΣREE (280–330 ppm) in the studied basaltic trachyandesites are rather low compared to CBVF rocks associated with the elevated concentrations of alkalis, P_2O_5, Sr, and REE (Fig. 8).

The chondrite-normalized concentrations of REE produce a smooth, moderately inclined patterns (La_N/Yb_N = 18.2–19.3; Fig. 9) with no Eu anomaly. The REE patterns correspond well to those of trachybasaltic and trachyandesitic rocks of the CSVC, whereas CBVF basalts have significantly higher concentrations of all REE.

Tab. 1 Major-element contents (wt. %) in the studied basaltic trachyandesites

Sample	JM01	JM02	JM03
Location	Holý vrch	Skalky	Hořidla
North	50.52980	50.53651	50.54048
East	14.23503	14.25027	14.26730
SiO_2	49.67	50.30	49.57
TiO_2	2.11	2.27	2.21
Al_2O_3	17.34	16.93	16.89
Fe_2O_3	3.45	3.45	3.62
FeO	4.44	4.53	4.26
MnO	0.20	0.19	0.19
MgO	2.55	2.64	2.62
CaO	7.70	7.59	7.75
Na_2O	4.33	4.40	4.43
K_2O	3.68	3.43	3.67
P_2O_5	0.563	0.535	0.550
H_2O^+	3.10	2.98	3.54
H_2O^-	0.23	0.24	0.26
F	0.111	0.108	0.100
CO_2	0.02	0.01	0.13
Total	99.48	99.60	99.80

4.5. K–Ar geochronology and Sr–Nd isotope composition

The measured Ar isotope ratios indicate that 56.3 % of the ^{40}Ar is radiogenic. With 2.94 wt. % of potassium (atomic), the calculated K–Ar age of sample JM02 is 29.12 ± 0.63 Ma (1σ; Tab. 3). Based on this age, the initial ratios of radiogenic isotope compositions were calculated: $^{87}Sr/^{86}Sr_i$ = 0.70475 and $^{143}Nd/^{144}Nd_i$ = 0.512700 (Tab. 3). These data resemble trachybasalts from the CSVC (Fig. 10; Ulrych et al. 2002; Ackerman et al. 2015), whereas they differ significantly from basanites of the same volcanic complex (Ulrych et al. 2002; Cajz et al. 2009).

5. Discussion

5.1. Magma emplacement

The field geological mapping, supported with LiDAR-based digital elevation model and ground magnetometric survey, suggests that with a single exception of the Křemín Hill the individual topographic peaks are interconnected to form a single 4.4 km long (SW–NE) and up to 2 km wide (NW–SE) intrusion. This assumption appears to be supported by ground magnetometry survey, which did not identify magma feeder for the largest occurrence at Hořidla to the northeast. The overall magnetometric image with negligible variations suggests the presence of a continuous magmatic body, with slightly varying thickness (irregular base and top), according to ground magnetometric survey. The two detected stronger anomalies (up to 1,275 nT) can be interpreted in terms of two narrow feeders (Holý vrch and Skalky hills) that supplied the sill with magma. The presence of a single larger intrusion is also supported by petrological data. The bulk-rock chemical composition, mineral proportions as well as composition of rock-forming minerals are rather homogeneous across all sampled outcrops except for the Křemín Hill.

The more disturbed magnetic image acquired for the Křemín Hill with a rapidly increasing and dropping intensity of the magnetic field supports the possibility of a small independent dike although no volcanic rocks crop out on the hill. The absence of natural outcrops may result from extensive construction works and building of a medieval fortification which might have consumed all local rock sources. The sample studied for petrography differs from the rocks of the main sill, suggesting that the Křemín dike is not directly connected with the sill.

Tab. 2 Trace-element concentrations (ppm) in the studied basaltic trachyandesites

Sample	JM01	JM02	JM03
Ba	949	900	842
Co	14.6	15.2	13.9
Cr	16	23	15
Cs	1.42	0.86	2.56
Cu	18.0	22.7	20.6
Ga	24.2	23.1	21.1
Hf	11.15	10.18	9.52
Nb	118.0	110.0	104.0
Ni	16	21	14
Pb	162	11.6	10.9
Rb	93.49	73.35	67.47
Sc	11.46	10.15	9.59
Sr	1082	940	919
Ta	7.45	6.79	6.36
Th	10.0	10.1	8.7
U	2.67	2.90	2.52
V	187	185	177
W	2.10	2.00	1.74
Zn	115	102	98
Zr	568	526	489
Y	30.81	27.97	26.19
La	73.1	68.0	62.6
Ce	150.5	138.7	128.7
Pr	15.99	14.66	13.19
Nd	55.6	51.0	47.7
Sm	9.43	8.63	8.10
Eu	2.80	2.58	2.46
Gd	8.13	7.41	6.91
Tb	1.09	0.99	0.92
Dy	5.63	5.04	4.72
Ho	1.07	0.95	0.89
Er	2.89	2.56	2.40
Tm	0.38	0.33	0.30
Yb	2.70	2.37	2.21
Lu	0.40	0.35	0.32

Cr and Ni by XRF, others by ICP-MS

5.2. Geochemistry and magma origin

Petrography of the studied rocks suggests that they do not represent primary magmas. Such assumption is supported by the chemical composition of the samples with low Mg# (37; [Mg# = 100 × Mg/(Mg + $Fe_{tot.}$) mol. %]), and low concentrations of compatible elements (15–23 ppm Cr, 14–21 ppm Ni). These data provide additional evi-

Tab. 3 Sr–Nd and K–Ar isotopic data from the studied basaltic trachyandesite

sample	$^{87}Sr/^{86}Sr_m$	2 se(M)	$^{87}Sr/^{86}Sr_{29}$	$^{143}Nd/^{144}Nd_m$	2 se(M)	$^{143}Nd/^{144}Nd_{29}$	K (%)	$^{40}Ar_{rad}$ (ccSTP/g)	$^{40}Ar_{rad}$ (%)	K/Ar age ± 1σ (Ma)
JM02	0.704867	47	0.704753	0.512719	6	0.512700	2.944	3.3596×10^{-6}	56.3	29.12 ± 0.63

Initial isotopic ratios were calculated to the age of 29 Ma

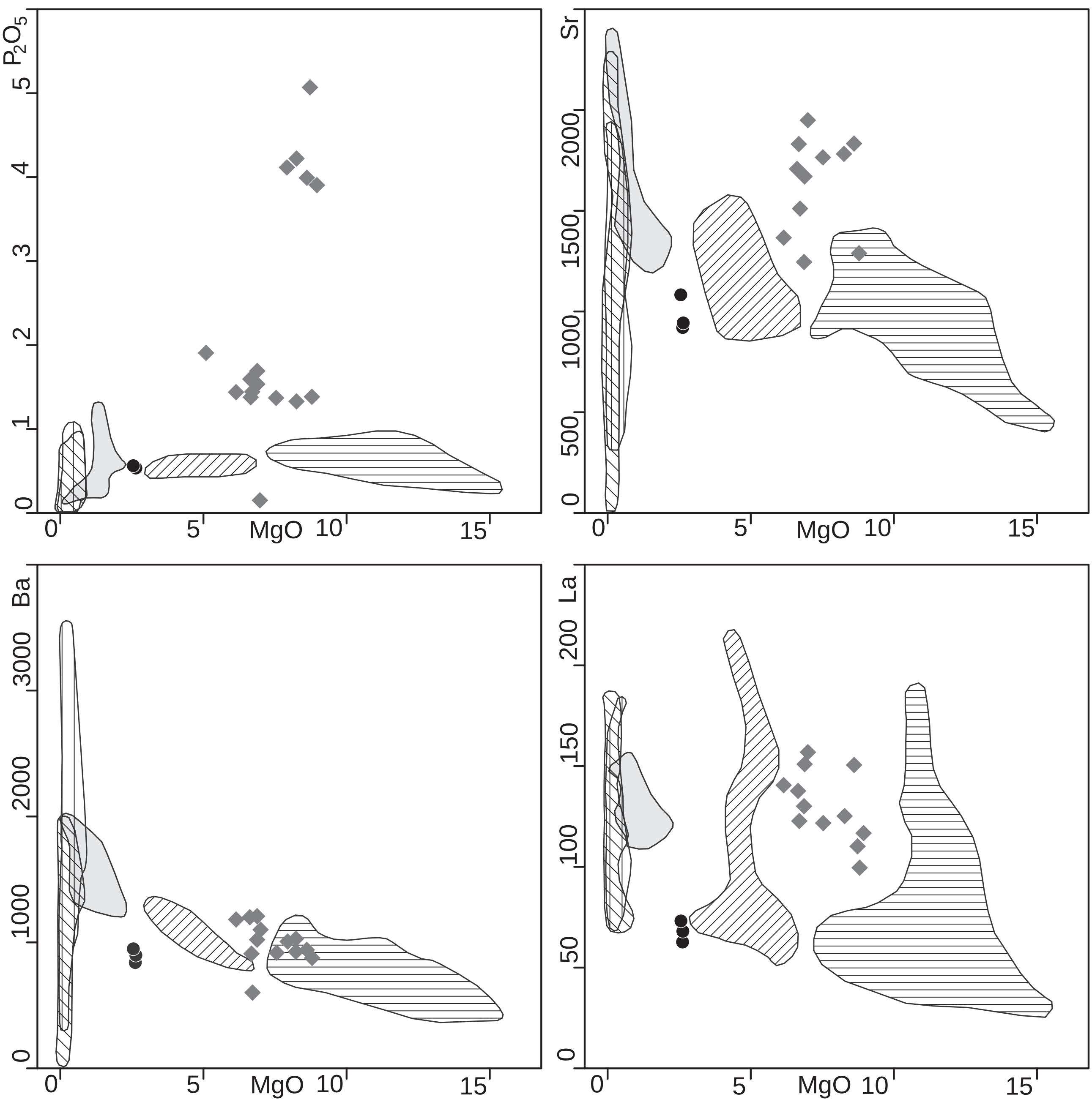

Fig. 8 Selected Fenner diagrams (MgO and P_2O_5 in wt. %, Sr, Ba, and La in ppm) for the studied rocks and published data from the České Středohoří Volcanic Complex (Ulrych et al. 2002; Ackerman et al. 2015) and the Central Bohemia Volcanic Field (Ulrych et al. 1998; Řanda et al. 2003; Jáklová et al. 2014). Symbols correspond to Fig. 7.

dence that Zahořany–Chotiněves basaltic trachyandesites do not belong to the Central Bohemia Volcanic Field that is characterized by generally elevated P_2O_5, Sr and REE contents (Fig. 8). Instead, the studied basaltic trachyandesites more closely fit the composition of weakly differentiated alkaline rocks of the České Středohoří Volcanic Complex, with major- and trace-element concentrations on the interpolated line between trachybasalts (Ulrych et al. 2002) and trachyandesites (Ackerman et al. 2015; Figs 7–8). Relation of the studied rocks to trachybasalt and trachyandesite is also significant, given parallel trends of chondrite-normalized REE concentrations (Fig. 9).

Even though few individual clinopyroxene phenocrysts display weak reverse zoning, commonly indicative of magma mixing (e.g., Nakagawa et al. 2002; Streck 2008; Tomiya et al. 2013; Rapprich et al. 2017b), most of the clinopyroxene crystal population evidenced common trend from Mg-rich (cores of larger phenocrysts) towards Fe-rich (phenocryst rims and groundmass microcrysts) members (Fig. 4). No signs of magma mixing were

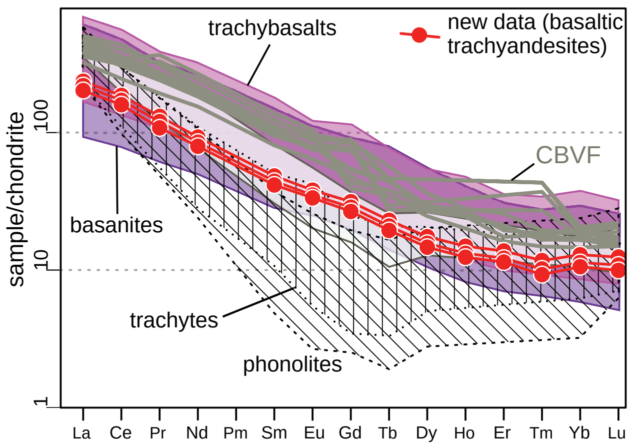

Fig. 9 Chondrite-normalized (Boynton 1984) spider-plot for the studied rocks and published data from the České Středohoří Volcanic Complex (Ulrych et al. 2002; Ackerman et al. 2015) and the Central Bohemia Volcanic Field (CBVF; Ulrych et al. 1998; Řanda et al. 2003; Jáklová et al. 2014). Symbols correspond to Fig. 7.

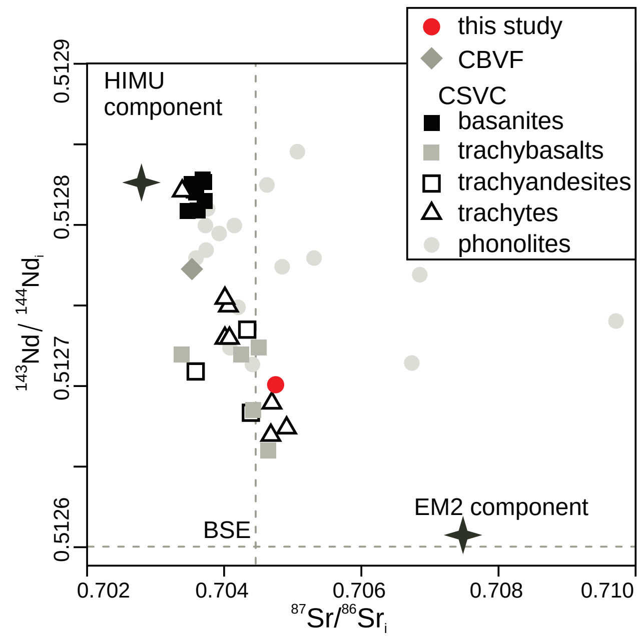

Fig. 10 Sr–Nd isotopic composition of sample JM02 compared with published data from České Středohoří Volcanic Complex (CSVC; Ulrych et al. 1998, 2002; Cajz et al. 2009; Ackerman et al. 2015) and Central Bohemia Volcanic Field (CBVF; Ulrych et al. 1998). Bulk Silicate Earth (BSE) after Faure (1986) for Sr and Jacobsen and Wasserburg (1980) for Nd; isotopic composition of HIMU and EM2 reservoirs after Hart (1988), while Rb/Sr and Sm/Nd values are averages from the compilation of Willbold and Stracke (2006). All data recast to initial values at 29 Ma.

observed in feldspars, with crystallization trend from labradorite (phenocrysts) towards sanidine (groundmass – Fig. 5), or in magnetite (with decreasing Mg admixture towards late smaller crystals in groundmass – Fig. 6). Overall textures and compositional zoning of rock-forming minerals document the origin of studied basaltic trachyandesites through fractional crystallization rather than by mixing of two distinct magma batches.

Tab. 4 Numeric model of fractional crystallization: **a** – derivation of studied basaltic trachyandesite (JM01) from trachybasalt (sample 1358 in Ulrych et al. 2002), chemistries of potentially fractionating minerals from Cajz et al. (2009); **b** – fractionation of studied basaltic trachyandesite (JM01) to trachyandesite (Ackerman et al. 2015), mineral chemistries from this study.

a – trend trachybasalt (1358: Ulrych et al. 2002) − basaltic trachyandesite JM01; degree of fractional crystallization 58 %; $\Sigma R^2 = 0.595$

	Parent (1358)	Cpx (41 %)	Pl (39 %)	Mt (14 %)	Ol (6 %)	Daughter (JM01)	Parent calculated	Difference	Cumulate
SiO_2	44.58	49.20	51.75	0.00	41.43	49.67	44.66	0.08	41.02
TiO_2	3.37	1.76	0.00	21.60	0.00	2.11	2.92	− 0.45	3.52
Al_2O_3	15.35	5.16	30.54	2.80	0.00	17.34	15.34	− 0.01	13.88
FeO_t	9.69	5.90	0.00	66.50	8.71	7.54	9.84	0.15	11.50
MgO	6.13	14.25	0.00	1.40	49.88	2.55	6.04	− 0.07	8.57
CaO	11.06	22.24	12.33	0.00	0.00	7.70	10.95	− 0.11	13.32
Na_2O	3.40	0.47	4.07	0.00	0.00	4.33	2.82	− 0.58	1.72
K_2O	1.63	0.00	0.00	0.00	0.00	3.68	1.55	− 0.08	0.00

b – trend basaltic trachyandesite JM01 − trachyandesite (171: Ackerman et al. 2015); degree of fractional crystallization 33 %; $\Sigma R^2 = 0.472$

	Parent (JM01)	Cpx (47 %)	Pl (34 %)	Mt (18 %)	Daughter (171)	Parent calculated	Difference	Cumulate
SiO_2	49.67	47.96	53.73	0.00	54.87	49.82	0.15	39.50
TiO_2	2.11	1.58	0.00	22.32	0.84	2.10	− 0.01	4.67
Al_2O_3	17.34	4.56	29.24	0.92	19.75	17.16	− 0.18	11.88
FeO_t	7.54	8.24	0.00	68.34	3.48	7.55	0.01	15.84
MgO	2.55	12.68	0.00	0.99	0.54	2.31	− 0.14	5.93
CaO	7.70	21.96	11.22	0.00	4.62	7.60	− 0.10	13.67
Na_2O	4.33	0.61	4.72	0.00	5.52	4.31	− 0.02	1.83
K_2O	3.68	0.00	0.37	0.00	4.54	3.09	− 0.59	0.12

The input data were the compositions of the representative trachybasalt (Ulrych et al. 2002), new data for basaltic trachyandesite (JM01), representative trachyandesite (Ackerman et al. 2015), and chemistries of the probably crystallizing mineral phases (from Cajz et al. 2009 and this study). The calculations were carried out for each of the fractionations steps separately, using the unpublished R-language plugin for the *GCDkit* software (Janoušek et al. 2016). ΣR^2 = sum of squared residuals.

The relations of the Zahořany–Chotiněves basaltic trachyandesite to known volcanic rocks from the České Středohoří Volcanic Complex was also tested using the Sr–Nd isotopic data. They fit well the range of Sr–Nd isotope compositions known from the trachybasalts and trachyandesites (Ulrych et al. 2002; Ackerman et al. 2015) but differ significantly from those reported for basanites (Ulrych et al. 2002; Cajz et al. 2009; Fig. 10). This could imply that basaltic trachyandesites were derived from trachybasalts by relatively closed-system fractional crystallization without detectable assimilation of crustal materials (e.g., Cretaceous sediments).

The possible derivation of basaltic trachyandesite from trachybasaltic magma was verified by least-squares major-element based modelling of fractional crystallization (Janoušek et al. 2016 and references therein). The composition of trachybasalt was adopted from Ulrych et al. (2002; sample 1358), chemistries of potentially fractionating minerals from Cajz et al. (2009). The observed composition (sample JM01) was obtained following 58% fractionation of 41 % clinopyroxene, 39 % plagioclase, 14 % titanomagnetite and 6 % olivine from a trachybasaltic melt (Tab. 4a).

A similar test was applied to further fractionation towards a trachyandesitic melt, using mineral chemistry data from this study. Following 33% fractionation of 47 % clinopyroxene, 34 % plagioclase and 18 % titanomagnetite, a composition comparable to the published trachyandesites (Ackerman et al. 2015) was reached (Tab. 4b).

The published data indicate a significant compositional change between basanites and trachybasalts, probably amplified by assimilation of ambient crustal rocks (Ackerman et al. 2015). In contrast, according to newly obtained data, the compositional shift between the trachybasalts and basaltic trachyandesites then appears to follow a simple fractional crystallization trend. In České Středohoří Volcanic Complex, significant assimilation most likely took place when large amounts of basanitic melts evolved to trachybasalts. In contrast, subordinate portions of trachybasaltic magmas evolving to basaltic trachyandesites and trachyandesites were less vulnerable to further assimilation of crustal rocks.

6. Conclusions

- The belt of basaltic trachyandesites between Zahořany and Chotiněves forms a single large sill with an irregular surface only partly exposed by selective erosion. This sill intruded at ~29 Ma and was most likely fed by two smaller conduits located underneath the Holý vrch and Skalky hills. The isolated occurrence at the Křemín Hill probably represents an independent intrusion with a slightly different petrography.
- Except for the isolated Křemín Hill, the remaining occurrences are compositionally homogeneous confirming the assumption of a single magmatic body.
- The composition of the basaltic trachyandesites from the studied sill (e.g., low P_2O_5 and Sr) suggests that this magmatic body belongs to the České Středohoří Volcanic Complex. The studied rocks fill the existing compositional gap between trachybasalts and trachyandesites known from the České Středohoří Volcanic Complex. Their position on the differentiation trend was confirmed by radiogenic isotope data and major-element modelling of crystal fractionation.

Acknowledgements. The work has been supported by the Czech Science Foundation project P210/12/1990, the Czech Geological Survey through the internal project 322800, and Isotope Climatology and Environmental Research Centre (ICER), Institute for Nuclear Research, Hungarian Academy of Sciences. The manuscript benefited from constructive comments by Francois Nauret, Etienne Medard and an anonymous reviewer, as well as handling editor Benjamin van Wyk de Vries and editor in chief Vojtěch Janoušek.

Electronic supplementary material. Supplementary tables with results of trace-element measurements in international standards, field documentation, ground magnetometry survey results as well as mineral chemistries of clinopyroxenes, feldspars and Fe–Ti oxides are available online at the Journal web site (***http://dx.doi.org/10.3190/jgeosci.278***).

References

Ackerman L, Ulrych J, Řanda Z, Erban V, Hegner E, Magna T, Balogh K, Frána J, Lang M, Novák JK (2015) Geochemical characteristics and petrogenesis of phonolites and trachytic rocks from the České Středohoří Volcanic Complex, the Ohře Rift, Bohemian Massif. Lithos 224: 256–271

Awdankiewicz M (2005) Reconstructing an eroded scoria cone: the Miocene Sośnica Hill Volcano (Lower Silesia, SW Poland). Geol Q 49: 439–448

Awdankiewicz M, Rapprich V, Míková J (2016) Magmatic evolution of compositionally heterogeneous monogenetic Cenozoic Strzelin Volcanic Field (Fore-Sudetic Block, SW Poland). J Geosci 61: 425–450

Balogh K (1985) K/Ar Dating of Neogene Volcanic Activity in Hungary: Experimental Technique, Experiences and Methods of Chronologic Studies. ATOMKI Reports D/1: 277–288

Blaikie TN, Ailleres L, Betts PG, Cas RAF (2014) A geophysical comparison of the diatremes of simple and complex maar volcanoes, Newer Volcanics Province, south-eastern Australia. J Volcanol Geotherm Res 276: 64–81

Boynton WV (1984) Cosmochemistry of the rare earth elements: meteorite studies. In: Henderson P (ed) Rare Earth Element Geochemistry. Elsevier, Amsterdam–New York, pp 63–114

Büchner J, Tietz O (2012) Reconstruction of the Landeskrone Scoria Cone in the Lusatian Volcanic Field, Eastern Germany – long-term degradation of volcanic edifices and implications for landscape evolution. Geomorphology 151: 175–187

Büchner J, Tietz O, Viereck L, Suhr P, Abratis M (2015) Volcanology, geochemistry and age of the Lausitz Volcanic Field. Int J Earth Sci (Geol Rundsch) 104: 2057–2083

Cajz V, Valečka J (2010) Tectonic setting of the Ohře/Eger Graben between the central part of the České středohoří Mts. and the Most Basin, a regional study. J Geosci 55: 201–215

Cajz V, Vokurka K, Balogh K, Lang M, Ulrych J (1999) The České Středohoří Mts.: volcanostratigraphy and geochemistry. Geolines 9: 21–28

Cajz V, Rapprich V, Erban V, Pécskay Z, Radoň M (2009) Late Miocene volcanic activity in the České Středohoří mountains (Ohře/Eger Graben, northern Bohemia). Geol Carpath 60: 519–533

Chulliat A, Macmillan S, Alken P, Beggan C, Nair M, Hamilton B, Woods A, Ridley V, Maus S, Thomson A (2015) The US/UK World Magnetic Model for 2015–2020: Technical Report. National Geophysical Data Center, NOAA. DOI: 10.7289/V5TB14V7

Clague DA (1978) The oceanic basalt–trachyte association: an explanation of the Daly gap. J Geol 86: 739–743

Daly RA (1914) Igneous Rocks and Their Origin. McGraw-Hill, New York, pp 1–563

Dempírová L, Šikl J, Kašičková R, Zoulková V, Kříbek B (2010) The evaluation of precision and relative error of the main components of silicate analyses in Central Laboratory of the Czech Geological Survey. Zpr geol výzk v r 2009: 326–330 (in Czech)

De Ritis R, Blanco-Montenegro I, Ventura G, Chiappini M (2005) Aeromagnetic data provide new insights on the volcanism and tectonics of Vulcano Island and offshore areas (southern Tyrrhenian Sea, Italy). Geophys Res Lett 32: L15305. DOI: 10.1029/2005GL023465

Dèzes P, Schmid SM, Ziegler PA (2004) Evolution of the European Cenozoic Rift System: interaction of the Alpine and Pyrenean orogens with their foreland lithosphere. Tectonophysics 389: 1–33

Domas S (ed 1988) Geological map of the Czech Republic, sheet 02-43 Litoměřice. Czech Geological Survey, Prague

Faure G (1986) Principles of Isotope Geology, second edition. John Wiley and Sons, London, pp 1–589

Haase KM, Beier C, Regelous M, Rapprich V, Renno A (2017) Spatial variability of source composition and petrogenesis in rift and rift flank alkaline lavas from the Eger Rift, Central Europe. Chem Geol 455: 304–314

Hamelin C, Seitz H-M, Barrat J-A, Dosso L, Maury RC, Chaussidon M (2009) A low δ^{7}Li lower crustal component: evidence from an alkalic intraplate volcanic series (Chaîne des Puys, French Massif Central). Chem Geol 266: 214–226

Hart SR (1988) Heterogeneous mantle domains: signatures, genesis and mixing chronologies. Earth Planet Sci Lett 90: 273–296

Holub FV, Rapprich V, Erban V, Pécskay Z, Mlčoch B, Míková J (2010) Petrology and geochemistry of the Tertiary alkaline intrusive rocks at Doupov, Doupovské hory Volcanic Complex (NW Bohemian Massif). J Geosci 55: 251–278

Jacobsen SB, Wasserburg GJ (1980) Sm–Nd isotopic evolution of chondrites. Earth Planet Sci Lett 50: 139–155

Jáklová K, Trubač J, Magna T, Rapprich V, Haloda J, Erban V (2014). Petrography, geochemistry and post-eruption phenomena of the olivine-poor apatite nephelinite from the Slánská hora Hill. Zpr geol výzk v r 2013: 115–119

Janoušek V, Moyen JF, Martin H, Erban V, Farrow C (2016) Geochemical Modelling of Igneous Processes – Principles and Recipes in R Language. Bringing the Power of R to a Geochemical Community. Springer-Verlag, Berlin, Heidelberg, pp 1–346

Jochum KP, Nohl U, Herwig K, Lammel E, Stoll B, Hofmann AW (2005) GeoReM: a new geochemical database for reference materials and isotopic standards. Geost Geoanal Res 29: 333–338

Jung S, Mezger K, Hauff F, Pack A, Hoernes S (2013) Petrogenesis of rift-related tephrites, phonolites and trachytes (Central European Volcanic Province, Rhön, FRG): constraints from Sr, Nd, Pb and O isotopes. Chem Geol 354: 203–215

Legendre C, Maury RC, Caroff M, Guillou H, Cotten J, Chauvel C, Bollinger C, Hémond C, Guille G, Blais S, Rossi P, Savanier D (2005) Origin of exceptionally abundant phonolites on Ua Pou Island (Marquesas, French Polynesia): partial melting of basanites followed by crustal contamination. J Petrol 46: 1925–1962

Le Bas MJ (1977) Carbonatite–Nephelinite Volcanism: An African Case History. John Wiley & Sons, London, pp 1–347

Le Maitre RW (ed), Streckeisen A, Zanettin B, Le Bas MJ, Bonin B, Bateman P, Bellieni G, Dudek A, Efremova S, Keller J, Lameyre J, Sabine PA, Schmid R, Sørensen H, Wooley AR (2002) Igneous Rocks. A Classification and Glossary of Terms. Recommendations of the International Union of Geological Sciences Subcommission on the Systematics of Igneous Rocks, 2nd Edition. Cambridge University Press, Cambridge–New York, pp 1–193

Le Roex AP, Cliff RA, Adair BJI (1990) Tristan da Cunha, South Atlantic: geochemistry and petrogenesis of a basanite–phonolite lava series. J Petrol 31: 779–812

Lugmair GW, Marti K (1978) Lunar initial $^{143}Nd/^{144}Nd$: differential evolution line of the lunar crust and mantle. Earth Planet Sci Lett 39: 349–357

Lustrino M, Wilson M (2007) The circum-Mediterranean anorogenic Cenozoic igneous province. Earth Sci Rev 81: 1–65

Marshall A, Connor C, Kruse S, Malservisi R, Richardson J, Courtland L, Connor L, Wilson J, Karegar MA (2015) Subsurface structure of a maar–diatreme and associated tuff ring from a high-resolution geophysical survey, Rattlesnake Crater, Arizona. J Volcanol Geotherm Res 304: 253–264

Maury RC, Brousse R, Villemant B, Joron J-L, Jaffrezic H, Treuil M (1980) Cristallisation fractionnée d'un magma basaltique alcalin: la série de la Chaîne des Puys (Massif Central, France). I. Pétrologie. Bull Minéral 103: 250–266

Mlčoch B, Konopásek J (2010) Pre-Late Carboniferous geology along the contact of the Saxothuringian and Teplá–Barrandian zones in the area covered by younger sediments and volcanics (western Bohemian Massif, Czech Republic). J Geosci 55: 81–94

Morimoto N (1988) Nomenclature of pyroxenes. Mineral Petrol 39: 55–76

Nakagawa M, Wada K, Wood CP (2002) Mixed magmas, mush chambers and eruption triggers: evidence from zoned clinopyroxene phenocrysts in andesitic scoria from the 1995 eruptions of Ruapehu volcano, New Zealand. J Petrol 43: 2279–2303

Odin GS (1982) Numerical Dating in Stratigraphy. John Wiley and Sons, New York, pp 1–1040

Pearce JA (1996) A user's guide to basalt discrimination diagrams. In: Wyman DA (ed) Trace Element Geochemistry of Volcanic Rocks: Applications for Massive Sulphide Exploration. Geological Association of Canada, Short Course Notes 12: 79–113

Petronis MS, Brister AR, Rapprich V, van Wyk de Vries B, Lindline J, Mišurec J (2015) Emplacement history of the Trosky basanitic volcano (Czech Republic): paleomagnetic, rock magnetic, petrologic, and anisotropy of magnetic susceptibility evidence for lingering growth of a monogenetic volcano. J Geosci 60: 129–147

Pin C, Gannoun A, Dupont A (2014) Rapid, simultaneous separation of Sr, Pb, and Nd by extraction chromatography prior to isotope ratios determination by TIMS and MC-ICP-MS. J Anal At Spectrom 29: 1858–1870

Rapprich V (2005) Compositional variation of clinopyroxenes of basaltic, essexitic and tephriphonolitic rocks from the Doupovské hory Volcanic Complex, NW Bohemia. J Czech Geol Soc 50: 119–132

Rapprich V, Holub FV (2008) Geochemical variations within the Upper Oligocene–Lower Miocene lava succession of Úhošť Hill (NE margin of Doupovské hory Mts., Czech Republic). Geol Q 52: 253–268

Rapprich V, Cajz V, Košťák M, Pécskay Z, Řídkošil T, Raška P, Radoň M (2007) Reconstruction of eroded monogenic Strombolian cones of Miocene age: a case study on character of volcanic activity of the Jičín Volcanic Field (NE Bohemia) and subsequent erosional rates estimation. J Geosci 52: 169–180

Rapprich V, Kochergina YV, Magna T, Laufek F, Halodová P, Bůzek F (2017a) Carbonate-rich dyke in Roztoky Intrusive Complex – an evidence for carbonatite magmatism in the Eger Rift? J Geosci 62: 121–136

Rapprich V, Shields S, Halodová P, Lindline J, van Wyk De Vries B, Petronis MS, Valenta J (2017b) Fingerprints of magma mingling processes within the Miocene Zebín tuff cone feeding system (Jičín Volcanic Field, Czech Republic). J Geosci 62: 215–229

Řanda Z, Novák JK, Balogh K, Frána J, Kučera J, Ulrych J (2003) Vinařická hora Hill Cenozoic composite volcano, Central Bohemia: geochemical constraints. Geolines 15: 126–132

Simonsen SL, Neumann E-R, Seim K (2000) Sr–Nd–Pb isotope and trace-element geochemistry evidence for a young HIMU source and assimilation at Tenerife (Canary Island). J Volcanol Geotherm Res 103: 299–312

Skácelová Z, Rapprich V, Valenta J, Hartvich F, Šrámek J, Radoň M, Gaždová R, Nováková L, Kolínský P, Pécskay Z (2010) Geophysical research on structure of partly eroded maar volcanoes: Miocene Hnojnice and Oligocene Rychnov volcanoes (northern Czech Republic). J Geosci 55: 333–345

Skála R, Ulrych J, Ackerman L, Jelínek E, Dostál J, Hegner E, Řanda Z (2014) Tertiary alkaline Roztoky Intrusive Complex, České Středohoří Mts., Czech Republic: petrogenetic characteristics. Int J Earth Sci (Geol Rundsch) 103:1233–1262

Steiger RH, Jäger E (1977) Subcommission on Geochronology; convention on the use of decay constants in geo- and cosmochronology. Earth Planet Sci Lett 36: 359–362

Stoppa F, Schiazza M (2013) An overview of monogenetic carbonatitic magmatism from Uganda, Italy, China and Spain: volcanologic and geochemical features. J South Am Earth Sci 41: 140–159

Streck MJ (2008) Mineral textures and zoning as evidence for open system processes. In: Putirka KD, Tepley F (eds) Minerals, Inclusions and Volcanic Processes. Mineralogical Society of America and Geochemical Society Reviews in Mineralogy and Geochemistry 69: 595–622

Tietz O, Büchner J (2015) The landscape evolution of the Lausitz Block since the Palaeozoic – with special emphasis to the neovolcanic edifices in the Lausitz Volcanic Field (Eastern Germany). Z Dt Ges Geowiss 166: 125–147

Tomiya A, Miyagi I, Saito G, Geshi N (2013) Short time scales of magma-mixing processes prior to the 2011 eruption of Shinmoedake volcano, Kirishima volcanic group, Japan. Bull Volcanol 75: 750

Ulrych J, Pivec E, Langrová A, Jelínek E, Arva-Sos E, Hohndorf A, Bendl J, Řanda Z (1998) Geochemically anomalous olivine-poor nephelinite of Říp Hill, Czech Republic. J Czech Geol Soc 43: 299–311

Ulrych J, Svobodová J, Balogh K (2002) The source of Cenozoic volcanism in the České Středohoří Mts., Bohemian Massif. Neu Jb Mineral, Abh 177: 133–162

Ulrych J, Dostál J, Adamovič J, Jelínek E, Špaček P, Hegner E, Balogh K (2011) Recurrent Cenozoic volcanic activity in the Bohemian Massif (Czech Republic). Lithos 123: 133–144

Ulrych J, Krmíček L, Tomek Č, Lloyd FE, Ladenberger A, Ackerman L, Balogh K (2016) Petrogenesis of Miocene alkaline volcanic suites from western Bohemia: whole rock geochemistry and Sr–Nd–Pb isotopic signatures. Chem Erde – Geochem 76: 77–93

Valečka J, Zelenka P, Mlčoch B, Cajz V, Rapprich V, Valigurský L, Kycl P, Šebesta J (2002) Slope movements hazards in the southeastern part of the České Středohoří Mts., in the area of Litoměřice county. Unpublished final report, Ministry of Environment, Prague, pp 1–28 (in Czech)

Valenta J, Rapprich V, Skácelová Z, Gaždová R, Fojtíková L (2014) The newly discovered Neogene maar volcano near the Mariánské Lázně, Western Bohemia. Acta Geodyn Geomater 11: 107–116

Vieten K, Hamm HM (1978) Additional notes "On the calculation of the crystal chemical formula of clinopyroxenes and their contents of Fe^{3+} from microprobe analyses. Neu Jb Mineral, Mh 2: 71–83

Villemant B, Joron J-L, Jaffrezic H, Treuil M, Maury RC, Brousse R (1980) Cristallisation fractionnée d'un magma basaltique alcalin: la série de la Chaîne des Puys (Massif Central, France). II. Géochimie. Bull Minéral 103: 267–286

Villemant B, Joron J-L, Jaffrezic H, Treuil M (1981) Distribution coefficients of major and trace elements: fractional crystallization in the alkali basalt series of Chaîne des Puys (Massif Central, France). Geochim Cosmochim Acta 45: 1997–2016

Walther D, Breitkreuz C, Rapprich V, Kochergina YV, Chlupáčová M, Lapp M, Stanek K, Magna T (2016) The Late Carboniferous Schönfeld–Altenberg Depression on the NW margin of the Bohemian Massif (Germany/Czech Republic): volcanosedimentary and magmatic evolution. J Geosci 61: 371–393

Wenger E, Büchner J, Tietz O, Mrlina J (2017) The polycyclic Lausche Volcano (Lausitz Volcanic Field) and its message concerning landscape evolution in the Lausitz Mountains (northern Bohemian Massif, Central Europe). Geomorphology 292: 193–210

Willbold M, Stracke A (2006) Trace element composition of mantle end-members: implications for recycling of oceanic and upper and lower continental crust. Geochem Geophys Geosyst 7: doi: 10.1029/2005GC001005

Woolley AR, Kjarsgaard BA (2008) Carbonatite occurrences of the world: map and database. Geological Survey of Canada, Open Files 5796, pp 1–28